Journal of Thermal Analysis and Calorimetry (2019) 135:1069–1079
https://doi.org/10.1007/s10973-018-7478-2

Experimental investigation on heat transfer enhancement for a ferrofluid in a helically coiled pipe under constant magnetic field

Abazar Abadeh[1] · Majid Mohammadi[1] · Mohammad Passandideh-Fard[1]

Received: 10 April 2018 / Accepted: 12 June 2018 / Published online: 21 June 2018

Abstract

This paper experimentally investigates the effects of constant magnetic field on the average Nusselt number variation when the water-based ferrofluid with 1 mass% Fe_3O_4 nanoparticles flows through a helically coiled pipe with constant wall temperature in various Reynolds numbers. The two-step method has been utilized for ferrofluid preparation. In order to increase the heat transfer coefficient of the system, both active and passive methods are employed simultaneously. Changing the pipe shape to a helical configuration and adding magnetic nanoparticles in the fluid flow are two passive methods, while the active method is the exertion of a magnetic field. The convective heat transfer coefficient and pressure drop are two basic criteria in the evaluation of the results, and the main geometrical parameters are curvature and torsion ratios. The effects of fluid flow rate and the strength of the magnetic fields are also investigated. Applying a 600 G constant magnetic field, the results show the average Nusselt number augmentation of nearly 7%. In constant Reynolds number, the stronger magnetic field of 900 G yields a higher average Nusselt number.

Keywords Helically coiled pipe · Ferrofluid · Magnetic field · Heat transfer enhancement

List of symbols

A	Area
C_p	Specific heat
$\bar{h}$	Average heat transfer coefficient
q_s	Heat transfer rate
ΔT_{lm}	Logarithmic temperature difference
$\dot{m}$	Mass flow rate
k	Conductivity
μ	Viscosity
ρ	Density
φ	Nanoparticles mass fraction in the base fluid
Nu	Nusselt number
Re	Reynolds number
f	Friction factor
T	Temperature
p	Coil pitch
d	Pipe diameter
D_c	Coil diameter
ΔP	Pressure drop
η	Dimensionless parameter for optimization
δ	Uncertainty

Subscripts

bf	Base fluid
nf	Nanofluid
b, o	Bulk, outlet
b, i	Bulk, inlet
w	Deionized water
c	Coil
ave	Average

✉ Mohammad Passandideh-Fard
mpfard@um.ac.ir

Abazar Abadeh
abazar.abadeh@mail.um.ac.ir

Majid Mohammadi
mohammadi.ma@mail.um.ac.ir

[1] Department of Mechanical Engineering, Ferdowsi University of Mashhad, Mashhad, Iran

Introduction

Nowadays, most industries employ various energy saving methods as much as possible duo to the increasing energy costs. Efforts have been made to enhance the heat transfer in heat exchangers, reduce the heat transfer duration, and consequently, improve the energy efficiency. Since heat exchangers are existed in many engineering applications such as power production, chemical industry, environment engineering, food industry, waste heat recovery,

refrigeration and air conditioning, heat transfer enhancement in these devices has drawn the attention of researchers [1].

In general, heat transfer enhancement is categorized into active and passive methods. Active methods are more effective, but they could be considerably expensive. Mechanical mixing, rotation, vibration, electrostatic field and magnetic field are classified as active methods. On the other hand, passive methods are not as effective as active techniques; however, they can be performed without further cost. Changing fluid properties, altering flow regime from laminar to turbulent and modifying the geometry of the setup, are the most applicable examples of passive methods [1, 2].

One of the passive methods that is very effective to enhance heat transfer rate can be the modification of the system geometry [3]. It has been shown that helical pipes used in many industrial applications increase the heat transfer due to the secondary flow induced by the centrifugal force [4, 5]. Several experimental studies investigated the effects of curvature and torsion ratios in helical pipes on heat transfer. Manlapaz and Churchill [6] studied the effect of torsion ratio in laminar flows in helical pipes. They found that when the coil pitch is lower than the coil radius, the effect of torsion ratio is negligible. Cioncolini and Santini [7] measured pressure drop for both laminar and turbulent flow regimes in different helical pipes. They concluded that as long as the effect of curvature ratio is considerable, the torsion ratio effect can be ignored. Huminic et al. [8] studied heat transfer characteristics of double-tube helical heat exchangers using nanofluids. They showed that increasing Dean number causes a major increment in convective heat transfer coefficient.

One of the other passive methods to improve heat transfer coefficient is adding solid nanoparticles to a fluid and altering its thermo-physical properties [9–11]. In the past decade, numerous studies have been conducted to investigate the heat transfer enhancement by using nanofluids in various geometries [3]. Akbaridoust et al. [12] experimentally and numerically studied the convective heat transfer of nanofluid in helically coiled pipes at constant wall temperature. They reported that increasing the curvature ratio of the coiled pipe increases both the heat transfer coefficient and pressure drop. Furthermore, they experimentally showed around 18 percent increase in the convective heat transfer coefficient in case of using CuO/water with a mass fraction of 0.1%. Moghadam et al. [13] studied the effects of CuO/water nanofluid on the efficiency of a flat-plate solar collector. They demonstrate that using 0.4% CuO/water nanofluid instead of water causes 16.7% improvement in solar collector efficiency. Dalvand and Moghadam [14] experimentally investigated a water/-nanofluid jacket performance in stack heat recovery. They showed that in case of using nanofluid with larger values of nanoparticle concentration, higher convective heat transfer in jacket is achieved.

Besides what previously mentioned, heat transfer characteristics can be enhanced by applying constant or alternating magnetic field to certain fluid flows. It is accepted that the thermo-physical properties of the ferrofluid change under the magnetic field. Gavili et al. [15] showed that the thermal conductivity of a ferrofluid under a constant magnetic field can be increased up to 200% at maximum value. Sundar et al. [16] had an experimental research on forced convection heat transfer and friction factor in a straight circular tube with Fe3O4 magnetic nanofluid. Motozawa et al. [17] studied the effect of magnetic field on heat transfer in rectangular duct laminar flow of a magnetic fluid. They achieved nearly 20% heat transfer enhancement by applying magnetic field. Zonouzi et al. [18] experimentally studied the effects of applying a magnetic quadrupole field on the convective heat transfer behavior and pressure drop of a water-based ferrofluid. They observed maximum enhancements of 23.4, 37.9 and 48.9% in the local heat transfer coefficient for the magnetic nanofluid in the presence of constant magnetic field. Ghofrani et al. [19] experimentally investigated the laminar forced convection heat transfer of ferrofluids under an alternating magnetic field. They reported an enhancement of convective heat transfer in the presence of the magnetic field. Azizian et al. [20] studied the effects of magnetic field on laminar convective heat transfer of magnetite nanofluids. They observed that when a magnetic field is applied, the local heat transfer coefficient of nanofluid is augmented up to 300%. Goharkhah et al. [21] experimentally studied convective heat transfer and hydrodynamic characteristics of a ferrofluid under an alternating magnetic field in a straight pipe. Based on their study, at a constant Reynolds number, a stronger magnetic field resulted in a larger heat transfer. Moreover, the influence of magnetic field is more pronounced in the thermally developing region. Bizhaem et al. [22] numerically studied the heat transfer of developing laminar nanofluid flow in helical tube. They reported that in comparison with the base fluid, using nanofluid shows better thermal performance at smaller Reynolds numbers in fully developed region. Ghadiri et al. [23] experimentally investigated a PVT system performance using nanoferrofluids. They indicated that in comparison with the value obtained for the same conditions with no magnetic field, an enhancement of about 4–5% in the overall efficiency occurs using an alternating magnetic field with 50 Hz frequency for 3 mass% ferrofluid,

As it is clear from the above literature review, studies on heat transfer enhancement in a pipe through the simultaneous use of active and passive methods are rare in the literature. In this study, therefore, both active and passive

methods are concurrently applied on a system to increase the heat transfer characteristics. Two passive methods are used, namely changing the shape of the pipe to a helical configuration and employing magnetic nanoparticles in the fluid flow. A magnetic field as an active method of heat transfer enhancement is also applied on the system. The investigation of the above three methods is performed using extensive experiments. Specifically, an experimental study on the use of Fe_3O_4 nanofluid in helically coiled pipes with different curvature and torsion ratios at a constant wall temperature in the presence of a magnetic field is the main contribution of this research. The convective heat transfer coefficient and pressure drop are two basic criteria in the evaluation of the results. Furthermore, the effects of fluid flow rate and the strength of the magnetic fields are investigated.

Experimental

Experimental setup

A schematic of the experimental apparatus is displayed in Fig. 1. The coiled pipe is put in a cubic chamber with dimension of 25 × 35 × 30 cm and is well insulated on the outside. The chamber is equipped with a temperature controlling system by which any desired uniform temperature, at the wall of the helical pipe, from ambient up to nearly 70 °C could be achieved. The helically coiled pipes are fabricated from circular straight copper pipes with a 2 m length, 6.5 mm inner diameter, 0.7 mm thickness and thermal conductivity of 385 W mK^{-1}. The thermal resistance of the pipe thickness is negligible. Table 1 provides various coiled pipes with different curvature and torsion ratios used in this study. The pipe diameter is constant in all cases. A photograph of the experiment setup used in this study is shown in Fig. 2.

To measure pressure drop between the inlet and outlet, two high precision pressure transmitters (BT 214 Pressure Transmitter, ATEK) are used. The value of pressure is read by the transmitter digital indicator. Two calibrated RTD PT 100 type thermocouples with an accuracy of 0.1 °C are utilized in order to measure the inlet and outlet bulk temperatures. The thermocouple sensor is put in the fluid flow. Each thermocouple is linked to a TC4Y indicator. The temperature controlling system is made of two heaters of 500 W, a TC4Y indicator, an RTD PT 100 thermocouple, and a SSR (solid-state relay). In this study, the controller is set at a temperature of 40 °C. The chamber temperature is shown by its indicator. If the temperature decreases from the desired temperature (40 °C), the TC4Y indicator sends a signal to the SSR to control the electric current so that the temperature remains constant at 40 °C. This controlling system is a PID controller.

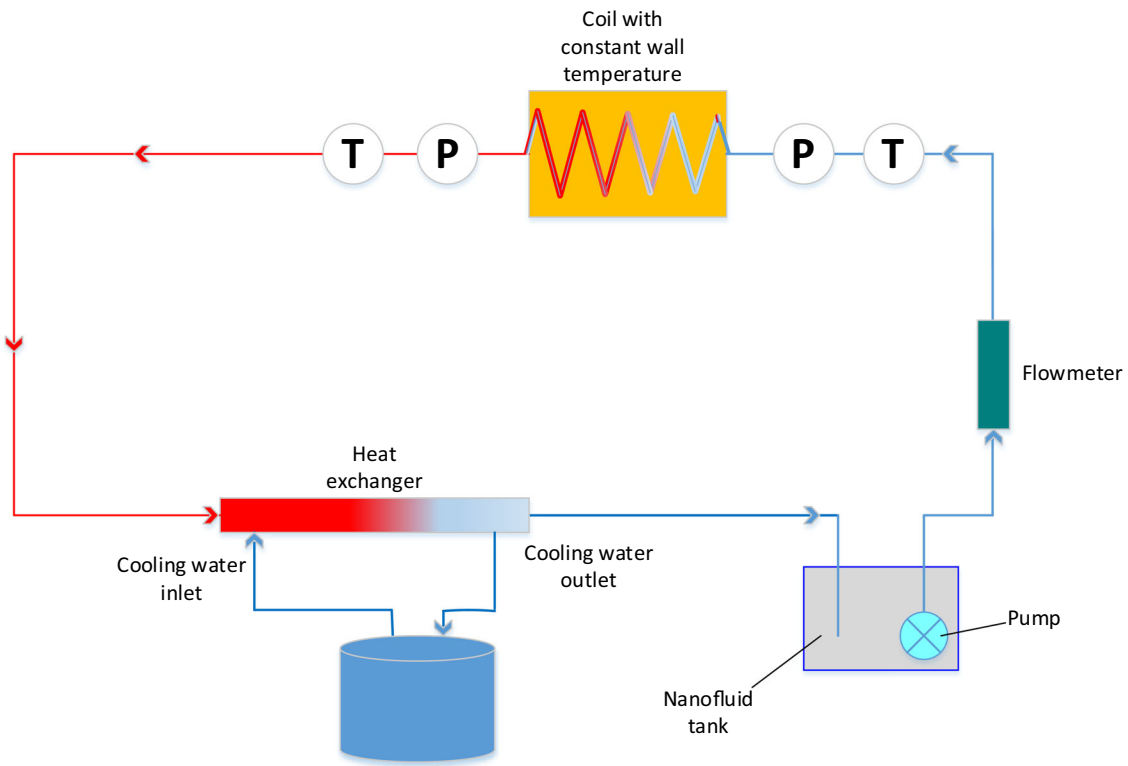

Fig. 1 A schematic of experimental setup

Table 1 Characteristics of helically coiled pipes

Coil number	Coil diameter D/mm	Total length L/cm	Coil pitch p/mm	δ	τ
Coil 1	95	200	30	0.068	0.100
Coil 2	135	200	30	0.048	0.070
Coil 3	170	200	30	0.038	0.056
Coil 4	220	200	30	0.030	0.043
Coil 5	135	200	20	0.048	0.047
Coil 6	135	200	40	0.048	0.093

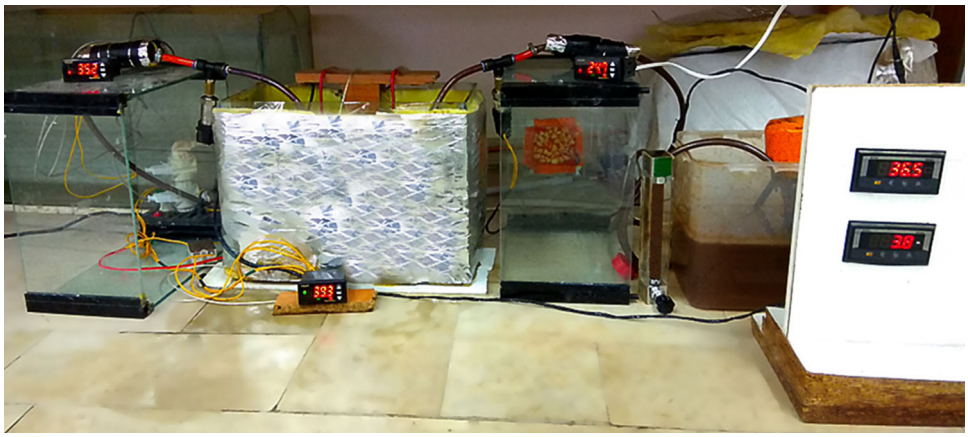

Fig. 2 A photograph of the experiment setup used in this study

The ferrofluid is driven from a reservoir tank through a calibrated flowmeter by a centrifugal pump. The volumetric flow rate is set by the flowmeter in the range of 10 to 60 L h^{-1} (LZB-10 glass tube rotameter). The heated ferrofluid exiting the coiled pipe enters a cooling section equipped with a concentric counter flow heat exchanger. The cold water is provided from another large tank with constant temperature.

A constant magnetic field is generated by four permanent neodymium magnets which are located at the top and bottom of the coil (as shown in Fig. 3). This orientation of the magnets provides a perpendicular magnetic field relative to local fluid flow direction. Each magnet has a size of 40 × 20 × 10 mm and a maximum strength of 900 Gauss measured by a Gauss meter (Lutron AC/DC Magnetic Meter (MG-3003SD) with Data Logging). The magnetic field is exerted to eight sections of the coil as shown in Fig. 3.

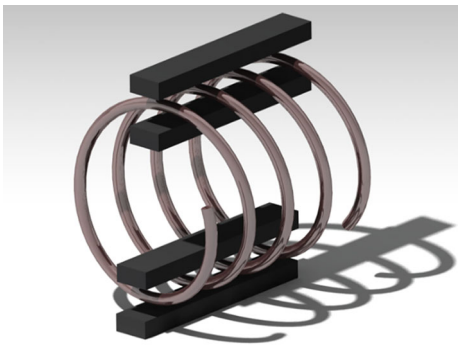

Fig. 3 A schematic of magnets positions

Nanofluid preparation

In this research, all chemicals are of the analytical grade (chemical grade) and used as-received without further treatment. All solutions are prepared with twice-distilled water. Citric acid (Merck, Germany) is selected as the surfactant. Fe_3O_4 nanoparticles are prepared from US Research Nanomaterials, Inc., USA. The purity of these nanoparticles is 98%, and their average diameter size is almost 20–30 nm. Generally, there are two methods for nanofluid preparation: one-step and two-step methods. In one-step method, the nanoparticles are synthesized in the base fluid and nanofluid is prepared. A two-step preparation process is accomplished through mixing base fluid with the obtained nanoparticles. Then, ultrasonic agitation, vigorous stirring, homogenizing, etc., are used to disperse the nanoparticles into the base fluid. The two-step method is the most extensively used one to prepare nanofluids and is more economical than the one-step method [24].

As shown in Fig. 4, Fe_3O_4 nanoparticles are grinded by a mortar to prevent or reduce agglomeration. Figures 5 and 6 show the TEM (transmission electron microscopy) image and DLS (dynamic light scattering) distribution of prepared nanoparticles, respectively. Based on the DLS distribution,

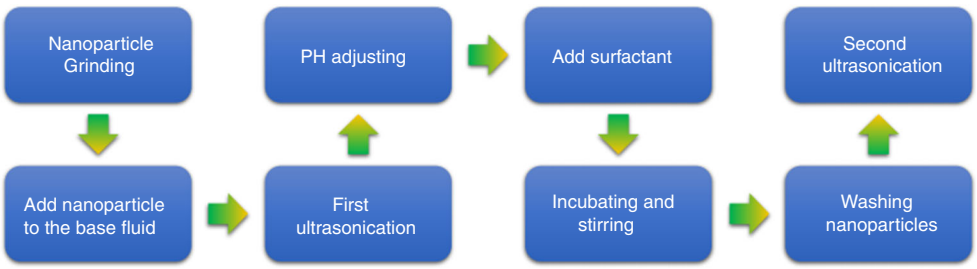

Fig. 4 A schematic of steps used for preparing nanofluids

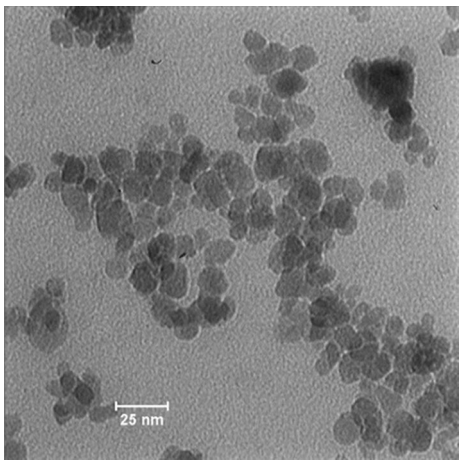

Fig. 5 A TEM image of Fe_3O_4

the mean diameter of the nanoparticles is 21.22 nm. Fe_3O_4 nanoparticles are added to the deionized water by one percent mass fraction, and the mixture is stirred manually for at least 5 min.

The prepared mixture is placed in the ultrasonic bath (Elma, Elmasonic, S60H, Germany) under sonication for an hour, with a frequency of 37 kHz, a power of 400 watts, under 100 percent amplitude and a temperature of 50 °C. The pH of the nanofluid is set at 11. Subsequently, the 2 M citric acid is added to the mixture and stirred manually. The prepared suspension is incubated in a hot plate heater stirrer (Corning PC-420D, USA) with a speed of 600 rpm for 60 min at 80 °C. Since the final suspension contains excess citric acid, the nanoparticles must be washed several times [25, 26]. Iridium magnets and deionized water have been used to accomplish the mentioned process. Finally, the suspension is put under sonication in the ultrasonic bath for 20 min with a temperature set at 50 °C.

There are several methods to investigate the final suspension (nanofluid) quality, such as the Zeta potential and magnetism tests, which are two methods utilized in this study. The Zeta potential is defined as the potential difference between the surface of nanoparticles immersed in a conducting liquid (water) and the bulk of the liquid. Zeta potential magnitude between 40 and 60 mV shows a well-stabilized nanofluid, while the greater magnitude shows better stabilization [24]. In the experiments performed in this study, the Zeta potential of the prepared nanofluid is 45.6 which is shown in Fig. 7.

The magnetism characteristic is another important criterion for a prepared ferrofluid [27]. A vibrating sample magnetometer (VSM) is used at room temperature in order to determine the magnetic characteristics of the prepared ferrofluid [26]. Figure 8 shows magnetic behavior of the prepared ferrofluid under magnetic field measured by VSM. As shown in this figure, Fe_3O_4 nanoparticles react to the change of the strength of magnetic field. As the magnetic field intensity approaches zero, the magnetism of the sample becomes zero, too. This means that by applying a magnetic field, Fe_3O_4 never becomes a magnet, and its

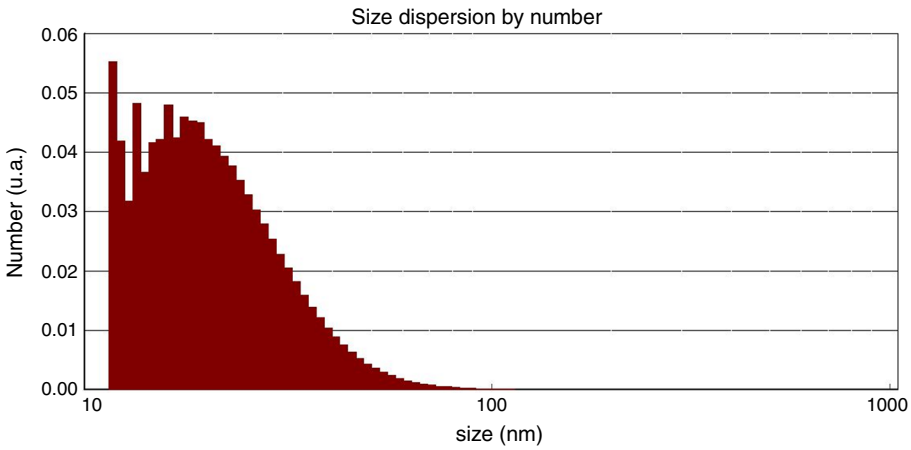

Fig. 6 A DLS report (particle size distribution) of nanoparticles

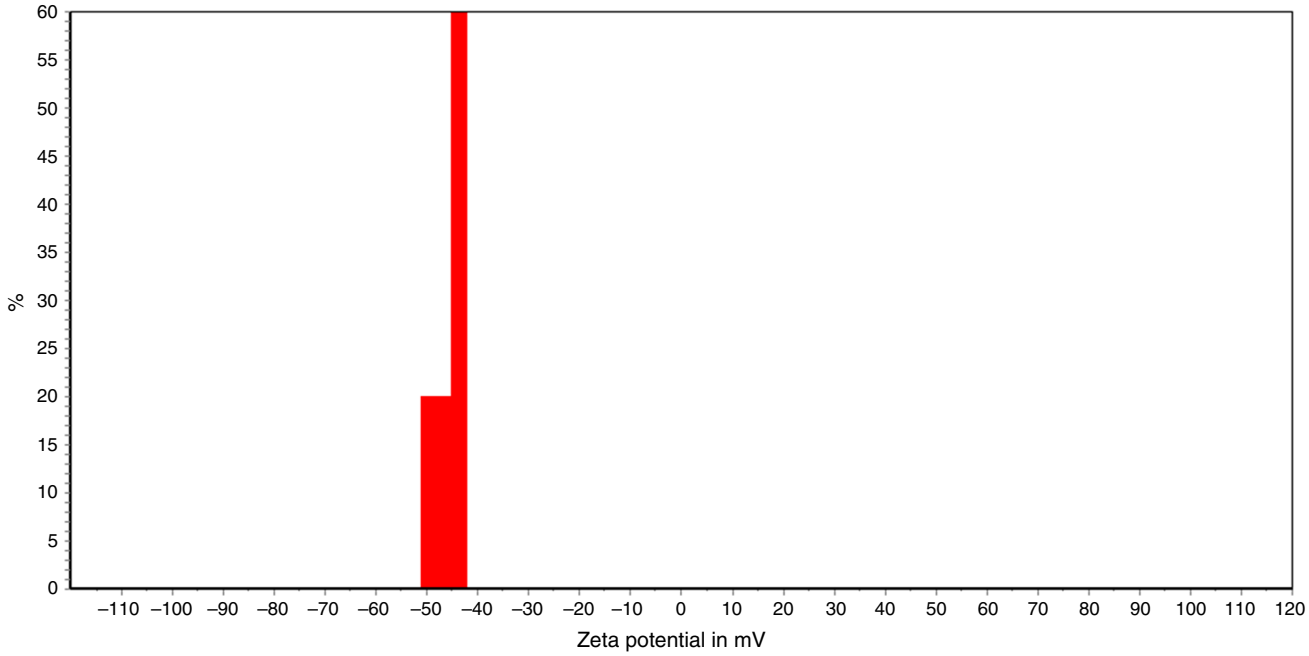

Fig. 7 A Zeta potential report

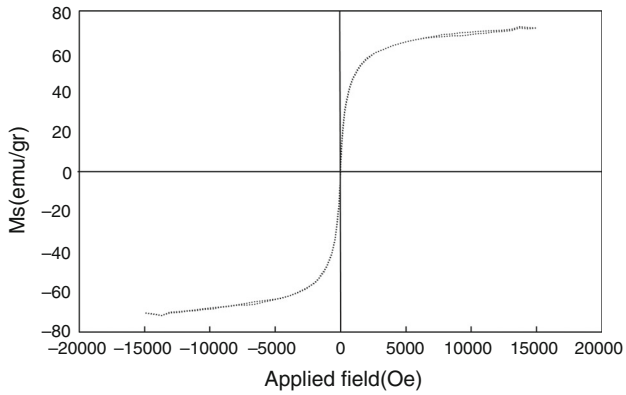

Fig. 8 A VSM report of the ferrofluid

magnetism residue is zero. This is very important that the nanoparticles never become magnets; otherwise, their deposition in the base occurs due to the aggregation.

Physical properties

Four main properties are density, viscosity, conductivity and heat capacity. Conductivity and heat capacity of ferrofluid samples are measured by KD2 Pro thermal properties analyzer (Decagon, USA, accuracy of 0.1%) and by the use of transient line heat source method. Ferrofluid density is measured by Densito 30PX portable specific density meter (Mettler Toledo, Switzerland, accuracy of 0.001 g cm^{-3}), and the viscosity of samples is measured by DVE viscometer (Brookfield, USA, accuracy of 1%). These properties for Fe_3O_4–water ferrofluid are measured and indicated in Table 2.

Measurements

To obtain average convective heat transfer coefficient, the amount of heat absorbed by the working fluid from the pipe with constant wall temperature is calculated as follows:

$$q_s = \dot{m} C_{p_{nf}} (T_{b,o} - T_{b,i}), \quad (1)$$

where $\dot{m}$ is the mass flow rate, $C_{p_{nf}}$ is the heat capacity of nanofluid, and $T_{b,i}$ and $T_{b,o}$ are the bulk temperatures at the inlet and outlet of the constant wall temperature pipe, respectively.

Having calculated q_s (amount of heat that the working fluid achieves), the average convective heat transfer coefficient is obtained as:

$$\bar{h} = q_s / A \Delta T_{lm} \quad (2)$$

which,

$$\Delta T_{lm} = (\Delta T_2 - \Delta T_1) / \ln(\Delta T_2 / \Delta T_1), \quad (3)$$

where ΔT_{lm} is the logarithmic mean temperature difference, $\bar{h}$ is the average convective heat transfer coefficient, $\Delta T_1 = T_{b,i} - T_s$, $\Delta T_2 = T_{b,o} - T_s$, and A is the inner lateral surface area of the pipe. Finally, the average Nusselt number and Reynolds number are calculated as:

Table 2 Measured thermo-physical properties

Fluid	Thermal conductivity/W m^{-1} K^{-1}	Viscosity/N s m^{-2}	Density/kg m^{-3}	Heat capacity/J kg^{-1} K^{-1}
Ferrofluid (1 mass%)	0.6867	0.00071	1005.62	4179
Pure water	0.6285	0.000654	993	4180

Table 3 Measurement devices, their information and uncertainty

Number	Instrument	Range	Measured parameter	Accuracy	Min and max measurable value	Relative uncertainty
1	PTD PT 100 thermocouple	0–200 C	Inlet and outlet temperature	0.1	24.5–41	0.244
2	Pressure transducer	0–100 mbar	Inlet and outlet pressure	0.1	1.5–42	0.238
3	Flow meter	0–70 L h^{-1}	Fluid flow rate	1	10–60	1.667
4	Geometry dimensions	1–20 mm	Pipe diameter and thickness	0.1	1–20	0.5
5	Physical properties	–	Conductivity, density, heat capacity, viscosity	–	–	0.1

$$Nu_{\text{ave}} = \frac{\bar{h}d}{k} \tag{4}$$

$$Re = \frac{4\dot{m}}{\pi d\mu}, \tag{5}$$

where k is the conductivity of the fluid. $\dot{m}$ is the mass flow rate, d is the pipe inner diameter, and μ is the dynamic viscosity of the fluid.

As it is shown, Eq. 6 computes the friction factor of a fluid inside a pipe.

$$f = \frac{\Delta P}{\left(\frac{l}{d}\right)\left(\frac{\rho V^2}{2}\right)}, \tag{6}$$

where ΔP is the pressure difference between inlet and outlet of the coil, l is the length of the pipe, d is the pipe diameter, ρ is the density of the nanofluid, and V is the nanofluid velocity in the pipe.

Uncertainty analysis

An error analysis is made to estimate the errors associated in the experimental results like Reynolds number and Nusselt number. The values of uncertainties estimated with different instruments are given in Table 3. For calculating the absolute uncertainty of Nusselt number, the following relation is employed [17].

$$\delta N = \sqrt{\left(\frac{\partial Nu}{\partial h}\delta h\right)^2 + \left(\frac{\partial Nu}{\partial D}\delta D\right)^2 + \left(\frac{\partial Nu}{\partial K}\delta K\right)^2} \tag{7}$$

and for the relative uncertainty:

$$\frac{\delta Nu}{Nu} = \sqrt{\left(\frac{\delta h}{h}\right)^2 + \left(\frac{\delta D}{D}\right)^2 + \left(\frac{\delta K}{K}\right)^2}. \tag{8}$$

Similarly, for other parameters, we have:

$$\frac{\delta \Delta T_{\text{lm}}}{\Delta T_{\text{lm}}} = \sqrt{\left(\frac{\delta T_{\text{b,i}}}{T_{\text{b,i}}}\right)^2 + \left(\frac{\delta T_{\text{b,o}}}{T_{\text{b,o}}}\right)^2 + \left(\frac{\delta T_{\text{s}}}{T_{\text{s}}}\right)^2} \tag{9}$$

$$\frac{\delta h}{h} = \sqrt{\left(\frac{\delta q_{\text{s}}}{q_{\text{s}}}\right)^2 + \left(\frac{\delta \Delta T_{\text{lm}}}{\Delta T_{\text{lm}}}\right)^2 + \left(\frac{\delta A}{A}\right)^2} \tag{10}$$

$$\frac{\delta Re}{Re} = \sqrt{\left(\frac{\delta \upsilon}{\upsilon}\right)^2 + \left(\frac{\delta d}{d}\right)^2 + \left(\frac{\delta v}{v}\right)^2}. \tag{11}$$

The maximum possible errors for the parameters involved in the analysis in this research are estimated and summarized in Table 4.

Results and discussion

Effect of coil diameter

Initially, the experiments are performed in a laminar flow with six different Reynolds numbers ($600 < Re < 2200$). First four coils configurations are given in Table 1. Figure 9 plots the average Nusselt number for the four coils versus the Reynolds numbers for deionized water as the working fluid. As seen from the figure, by increasing the Reynolds number and/or decreasing the coil diameter, the

Table 4 Uncertainty of different parameters

Parameter	Relative uncertainty
ΔT_{lm}	0.422
h	1.676
Re	1.670
Nu	1.708
q_s	1.796

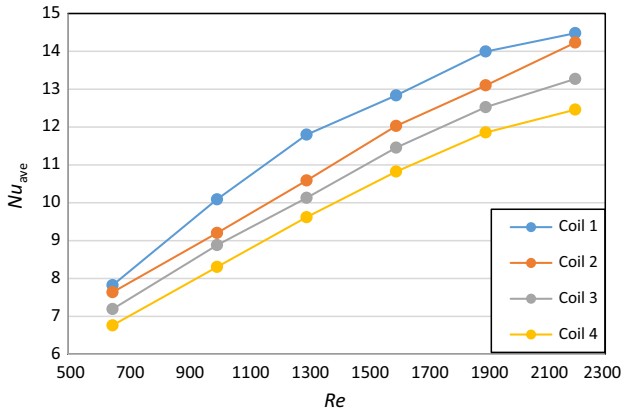

Fig. 9 Variation of the average Nusselt number versus the Reynolds number for the four coils with deionized water

average Nusselt number is enhanced. Decreasing coil diameter causes a higher centrifugal force applied to the fluid flowing through the coil. Higher centrifugal force makes the fluid to get more heat from the hot coil wall. In addition, because of higher density of nanoparticles compared to the base fluid, metallic oxide nanoparticles are more affected under centrifugal force, and therefore, these particles approach the wall and as a result, the less the coil diameter (D) is, the larger the average Nusselt number will be.

The curvature (δ) and torsion (τ) ratio are presented by Cioncolini et al. [7]

$$\delta = \frac{\pi^2 d D_c}{p^2 + \pi^2 D_c^2} \tag{12}$$

$$\tau = \frac{\pi d p}{p^2 + \pi^2 D_c^2}. \tag{13}$$

Figure 10 displays the friction factor for different coil diameters and Reynolds numbers measured using Eq. 6 by flowing water as the working fluid. Increasing the Reynolds number and the coil diameter decreases the friction factor. As seen in Figs. 9 and 10, increasing mass flow rate leads to increment in the heat transfer rate and also pressure drop. Furthermore, since the variations are not linear, a dimensionless parameter (η) is usually used in the

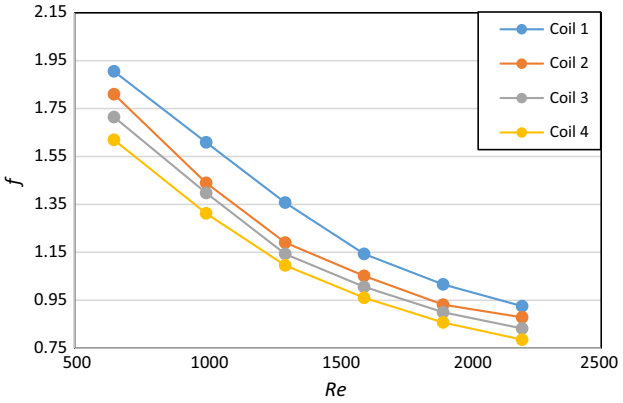

Fig. 10 Variation of the friction factor versus the Reynolds number for the four coils with deionized water

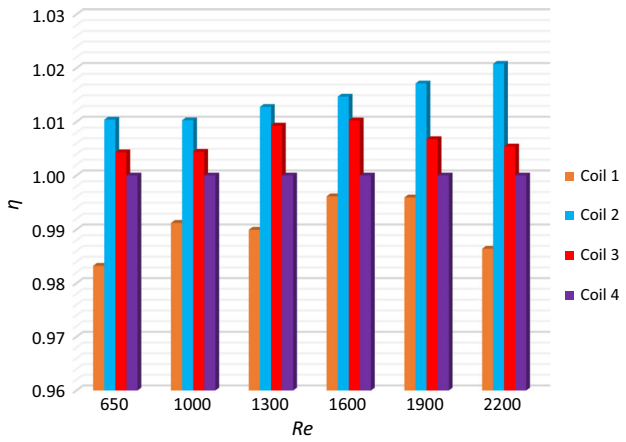

Fig. 11 η parameter for the four coils with deionized water in different Reynolds numbers

Table 5 Average Nusselt number and friction factor for Coil 4

Re	650	1000	1300	1600	1900	2200
Nu	6.97	8.41	9.77	11.01	12.09	12.74
f	1.83	1.40	1.15	1.00	0.90	0.83

literature, to compare the performance of different coils with respect to both heat transfer and pressure drop [3, 28].

$$\eta = \frac{\bar{h}/\bar{h}_{coil4}}{\Delta P/\Delta P_{coil4}}. \tag{14}$$

From Eq. 14, it could be easily understood that a coil with higher convective heat transfer coefficient and lower pressure drop have a better performance.

Figure 11 shows the value of η for all flow rates and coils when the working fluid is deionized water. The results for Coil 4, selected as the reference coil, are given in Table 5. As observed in Fig. 11, Coil 2 (2 m length, 6.5 mm inner diameter, 0.7 mm thickness, coil pitch of 30 mm, coil diameter of 135 mm, thermal conductivity of

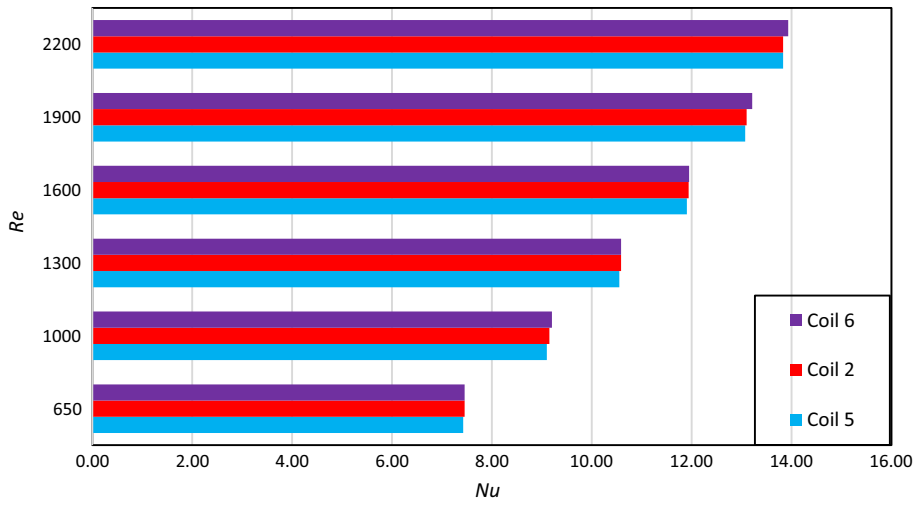

Fig. 12 Effect of coil pitch on average Nusselt number in Coil 2, Coil 5 and Coil 6 with deionized water

385 W mK^{-1} and η value of 1.02 at maximum state) has the highest η value for almost all flow rates in comparison with other three coils. As a result, the rest of the experiments are carried out with Coil 2.

The influence of the pipe torsion ratio is also investigated in this research. The pitch for Coil 2 is varied from 2 cm to 4 cm; the corresponding results for the average Nusselt number (Fig. 12) reveal that the effect of torsion ratio in the range studied in this research is not considerable.

Effect of using nanofluid and constant magnetic field

Due to the suspension of magnetic nanoparticles in the base fluid, the ferrofluid has a better heat transfer capability compared to that of deionized water [29]. Therefore, the ferrofluid flowing through the helically coiled pipe leads to a higher average Nusselt number.

Figure 13 presents the enhancement of average Nusselt number when using 1 mass% Fe_3O_4 ferrofluid in comparison with that of deionized water. Higher thermal

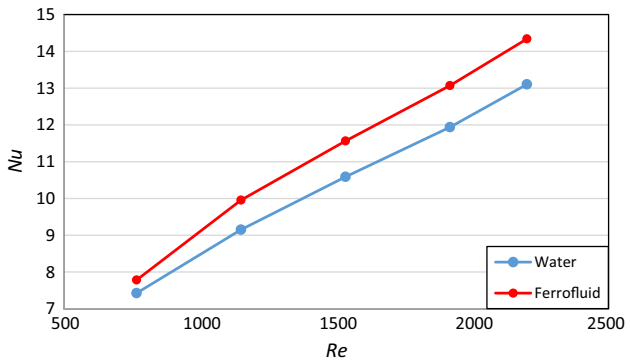

Fig. 13 Effect of using 1 mass% Fe_3O_4–water nanofluid in Coil 2

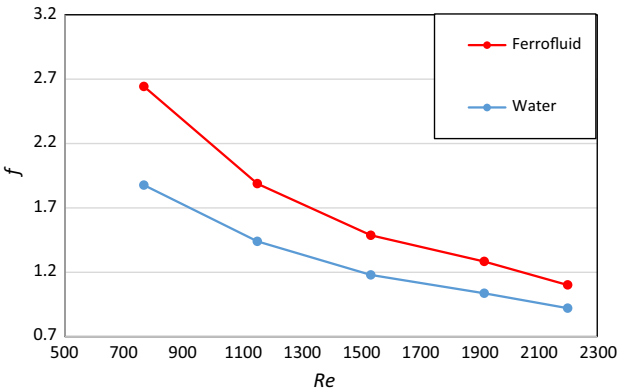

Fig. 14 Comparison of friction factor in Coil 2 for deionized water and ferrofluid

conductivity of nanofluid in comparison with that of the base fluid along with Brownian and thermophoresis effects are some reasons for enhancement of average Nusselt number. This heat transfer augmentation is observed for all flow rates in the selected Coil 2. The friction factor of Fe_3O_4 ferrofluid and deionized water is also illustrated in Fig. 14. Obviously, the friction factor for both deionized water and ferrofluid is reduced by increasing the Reynolds number. The difference between the friction factor of deionized water and ferrofluid decreases with increasing the Reynolds numbers.

The enhancement of average Nusselt number for Coil 2 compared to that of the reference coil (Coil 4) is depicted in Fig. 15. The results show that higher Reynolds numbers cause more enhancement of the average Nusselt number in a laminar flow.

The effect of applying two constant magnetic fields in Coil 2 for ferrofluid is displayed in Fig. 16. As seen from the figure, by applying a constant magnetic field of 600 G, the average Nusselt number increases by nearly 7%. Furthermore, at a constant Reynolds number, exerting a

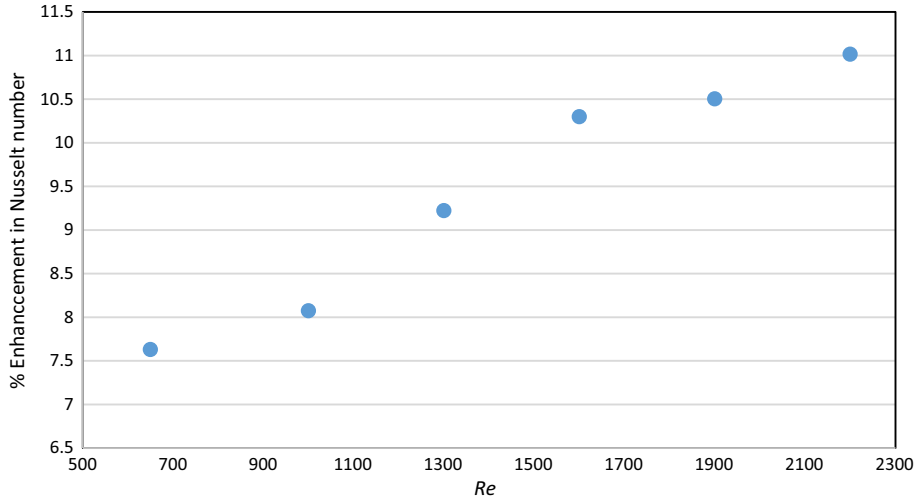

Fig. 15 Effect of the Reynolds number on the Nusselt number enhancement of ferrofluid in Coil 2 in comparison with that of the reference coil (Coil 4)

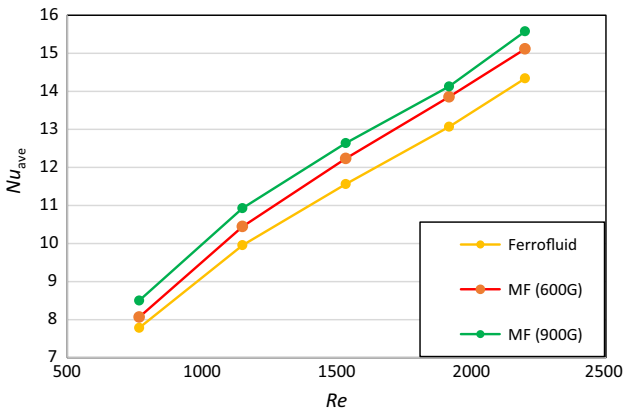

Fig. 16 Effect of applying a constant magnetic field in Coil 2 for ferrofluid

Table 6 Effect of a constant magnetic field on the average Nusselt number enhancement at different Reynolds numbers

Re	650	1000	1300	1600	1900	2200
600 G	3.6	4.9	5.8	6.0	5.4	6.2
900 G	9.2	9.8	9.3	8.1	8.6	9.7

stronger magnetic field (900 G) yields a higher average Nusselt number.

Table 6 provides the heat transfer enhancement by using 600 G and 900 G magnetic fields compared to the case with no magnetic field. The existence of magnetic field has a positive effect on heat transfer and can improve the average Nusselt number up to almost 10% in the range studied in this research.

Having a major effect on local concentration of nanoparticles dispersed in the base fluid, a magnetic field forces the nanoparticles move to the wall, which changes the fluid flow behavior. Therefore, magnetic field helps nanofluid to have a better heat transfer behavior due to Brownian and thermophoresis mechanisms.

Conclusions

This paper involves experimental investigation of the effects of applying ferrofluid as working fluid and also constant magnetic field on the average Nusselt number behavior of the water-based ferrofluid with 1 mass% Fe_3O_4 flowing through a helically coiled pipe with constant wall temperature in different Reynolds numbers. Fe_3O_4 nanoparticles are added to the deionized water, and quality of prepared ferrofluid is checked with Zeta potential and magnetism criteria.

The effect of curvature on the heat transfer is studied by examining the heat transfer in curved pipes with a constant length and different radii of curvature. It is shown that curved pipes are capable of enhancing the heat transfer with more augmentation for those with smaller radius of curvature. Investigating the influence of the pipe torsion ratio, it is concluded that the effect of torsion ratio in the range studied in this research is not considerable.

In order to study the effect of magnetic field on heat transfer, two constant magnetic fields of 600 and 900 G were applied to the flow. The results show that by applying the magnetic field of 600 G, the average Nusselt number increases by nearly 7%. Furthermore, at constant Reynolds number, exerting the stronger magnetic field (900 G) yields a higher average Nusselt number. As a conclusion, the existence of magnetic field has a positive effect on heat transfer and can improve the average Nusselt number up to almost 10% in the range studied in this research.

References

1. Huminic G, Huminic A. Application of nanofluids in heat exchangers: a review. Renew Sustain Energy Rev. 2012;16:5625–38.
2. Wen D, Lin G, Vafaei S, Zhang K. Review of nanofluids for heat transfer applications. Particuology. 2009;7:141–50.
3. Rakhsha M, Akbaridoust F, Abbassi A, Majid S-A. Experimental and numerical investigations of turbulent forced convection flow of nano-fluid in helical coiled tubes at constant surface temperature. Powder Technol. 2015;283:178–89.
4. Suresh S, Chandrasekar M, Selvakumar P. Experimental studies on heat transfer and friction factor characteristics of CuO/water nanofluid under laminar flow in a helically dimpled tube. Heat Mass Transf. 2012;48:683–94.
5. Xin R, Ebadian M. The effects of Prandtl numbers on local and average convective heat transfer characteristics in helical pipes. J Heat Transf. 1997;119:467–73.
6. Manlapaz RL, Churchill SW. Fully developed laminar flow in a helically coiled tube of finite pitch. Chem Eng Commun. 1980;7:57–78.
7. Cioncolini A, Santini L. An experimental investigation regarding the laminar to turbulent flow transition in helically coiled pipes. Exp Therm Fluid Sci. 2006;30:367–80.
8. Huminic G, Huminic A. Heat transfer characteristics in double tube helical heat exchangers using nanofluids. Int J Heat Mass Transf. 2011;54:4280–7.
9. Zhu H, Han D, Meng Z, Wu D, Zhang C. Preparation and thermal conductivity of CuO nanofluid via a wet chemical method. Nanoscale Res Lett. 2011;6:181.
10. Yu W, France DM, Routbort JL, Choi SU. Review and comparison of nanofluid thermal conductivity and heat transfer enhancements. Heat Transf Eng. 2008;29:432–60.
11. Pang C, Jung J-Y, Kang YT. Thermal conductivity enhancement of Al2O3 nanofluids based on the mixtures of aqueous NaCl solution and CH3OH. Int J Heat Mass Transf. 2013;56:94–100.
12. Akbaridoust F, Rakhsha M, Abbassi A, Saffar-Avval M. Experimental and numerical investigation of nanofluid heat transfer in helically coiled tubes at constant wall temperature using dispersion model. Int J Heat Mass Transf. 2013;58:480–91.
13. Moghadam AJ, Farzane-Gord M, Sajadi M, Hoseyn-Zadeh M. Effects of CuO/water nanofluid on the efficiency of a flat-plate solar collector. Exp Therm Fluid Sci. 2014;58:9–14.
14. Dalvand HM, Moghadam AJ. Experimental investigation of a water/nanofluid jacket performance in stack heat recovery. J Therm Anal Calorim. 2018. https://doi.org/10.1007/s10973-018-7220-0
15. Gavili A, Zabihi F, Isfahani TD, Sabbaghzadeh J. The thermal conductivity of water base ferrofluids under magnetic field. Exp Therm Fluid Sci. 2012;41:94–8.
16. Sundar LS, Naik M, Sharma K, Singh M, Reddy TCS. Experimental investigation of forced convection heat transfer and friction factor in a tube with Fe3O4 magnetic nanofluid. Exp Therm Fluid Sci. 2012;37:65–71.
17. Motozawa M, Chang J, Sawada T, Kawaguchi Y. Effect of magnetic field on heat transfer in rectangular duct flow of a magnetic fluid. Phys Proc. 2010;9:190–3.
18. Zonouzi SA, Khodabandeh R, Safarzadeh H, Aminfar H, Trushkina Y, Mohammadpourfard M, et al. Experimental investigation of the flow and heat transfer of magnetic nanofluid in a vertical tube in the presence of magnetic quadrupole field. Exp Therm Fluid Sci. 2018;91:155–65.
19. Ghofrani A, Dibaei M, Sima AH, Shafii M. Experimental investigation on laminar forced convection heat transfer of ferrofluids under an alternating magnetic field. Exp Thermal Fluid Sci. 2013;49:193–200.
20. Azizian R, Doroodchi E, McKrell T, Buongiorno J, Hu L, Moghtaderi B. Effect of magnetic field on laminar convective heat transfer of magnetite nanofluids. Int J Heat Mass Transf. 2014;68:94–109.
21. Goharkhah M, Ashjaee M, Shahabadi M. Experimental investigation on convective heat transfer and hydrodynamic characteristics of magnetite nanofluid under the influence of an alternating magnetic field. Int J Therm Sci. 2016;99:113–24.
22. Bizhaem HK, Abbassi A. Numerical study on heat transfer and entropy generation of developing laminar nanofluid flow in helical tube using two-phase mixture model. Adv Powder Technol. 2017;28:2110–25.
23. Ghadiri M, Sardarabadi M, Pasandideh-fard M, Moghadam AJ. Experimental investigation of a PVT system performance using nano ferrofluids. Energy Convers Manag. 2015;103:468–76.
24. Jama M, Singh T, Gamaleldin SM, Koc M, Samara A, Isaifan RJ, Atieh MA. Critical review on nanofluids: preparation characterization and applications. J Nanomater. 2016. https://doi.org/10.1155/2016/6717624
25. Cheraghipour E, Tamaddon A, Javadpour S, Bruce I. PEG conjugated citrate-capped magnetite nanoparticles for biomedical applications. J Magn Magn Mater. 2013;328:91–5.
26. Cheraghipour E, Javadpour S, Mehdizadeh AR. Citrate capped superparamagnetic iron oxide nanoparticles used for hyperthermia therapy. J Biomed Sci Eng. 2012;5:715.
27. Odenbach S. Ferrofluids: magnetically controllable fluids and their applications, vol. 594. Berlin: Springer; 2008.
28. Akhavan-Behabadi M, Pakdaman MF, Ghazvini M. Experimental investigation on the convective heat transfer of nanofluid flow inside vertical helically coiled tubes under uniform wall temperature condition. Int Commun Heat Mass Transf. 2012;39:556–64.
29. Naphon P, Wiriyasart S, Arisariyawong T, Nualboonrueng T. Magnetic field effect on the nanofluids convective heat transfer and pressure drop in the spirally coiled tubes. Int J Heat Mass Transf. 2017;110:739–45.